FAR-INFRARED RADIATIVE PROPERTIES OF WATER VAPOR AND CLOUDS IN ANTARCTICA

BY LUCA PALCHETTI, GIOVANNI BIANCHINI, GIANLUCA DI NATALE, AND MASSIMO DEL GUASTA

Two years of spectral infrared measurements of downwelling radiation between 7 and 100 μm in wavelength at high altitude over the Antarctic Plateau are presented.

Water vapor and clouds are among the most important components of the atmosphere that modulate the Earth radiation budget by means of the strong contributions to the greenhouse effect and the planetary albedo. They trap a significant amount of the longwave thermal infrared radiation emitted by the underlying atmosphere and the surface (greenhouse effect) and reflect back to space the shortwave solar incoming radiation (albedo effect). Water vapor and clouds are not usually considered to be causes of anthropogenic climate forcing, but instead they are critical components of feedback processes owing to their strong greenhouse effect (Stocker et al. 2014). They are recognized as fundamental components whose radiative properties, and their associated impact on the radiation budget, must be better understood to improve climate predictions. Nevertheless, while broadband observations that can determine the overall radiative impact are performed, the radiative properties of water vapor and clouds are underexplored since spectrally resolved measurements, able to link the radiative impact to the underlying components, are missing.

Most uncertainties that are present in the characterization of the longwave emission of the atmosphere come from the lack of spectrally resolved measurements in the far-infrared (FIR) spectral region from 100 to 667 cm^{-1} (100–15 μm) (Turner and Mlawer 2010). Even though the FIR spectral region contains more than 40% of the total longwave energy emitted by Earth, and about 60% of the associated radiative cooling occurs in the FIR (Clough et al. 1992), there have been only a few spectral measurements and datasets collected in this region [see Harries et al. (2008) for an in-depth discussion]. This is partially explained by 1) a lack of spaceborne spectrometers operating in the FIR—in the 1970s only there was a very early spaceborne sensor, the Infrared Interferometer Spectrometer (IRIS) on board the *Nimbus-3* and *-4* satellites, that provided relatively low-resolution

AFFILIATIONS: PALCHETTI, BIANCHINI, DI NATALE, AND DEL GUASTA—Consiglio Nazionale delle Ricerche, Istituto Nazionale di Ottica, Florence, Italy
CORRESPONDING AUTHOR: Luca Palchetti, Consiglio Nazionale delle Ricerche, Istituto Nazionale di Ottica, Via Madonna del Piano 10, Sesto Fiorentino 50019, Italy
E-mail: luca.palchetti@ino.it

The abstract for this article can be found in this issue, following the table of contents.
DOI:10.1175/BAMS-D-13-00286.1

In final form 16 March 2015

spectra across a portion of the FIR (Conrath et al. 1970), and currently even if there are a few missions under study, none of them are still deployed in space (Rizzi et al. 2002; Mlynczak et al. 2002)—and 2) that ground-based observations are hampered by the strong water vapor absorption in this spectral region and, thus, meaningful ground-based observations can only be made in high altitude or very dry locations (as described in this paper) or from stratospheric balloons (Palchetti et al. 2006; Mlynczak et al. 2006a,b).

As for water vapor spectroscopy, there are still some uncertainties in the FIR concerning the knowledge of the line shape for frequencies far from the center of the lines. The contribution of this component to the total absorption of the water vapor is known as the "continuum absorption" and has a strong impact on the total water vapor absorption. An in-depth discussion about the importance of the characterization in the FIR spectral region and a clear explanation of the continuum absorption can be found in Turner and Mlawer (2010).

Also the radiative properties of ice particles in clouds, such as cirrus or polar stratospheric clouds (PSC), are not well known in the FIR and only a few models were developed to cover this spectral region (Yang et al. 2003, 2013). The FIR spectral range will provide unique information about cirrus clouds. Since the radiative properties of the ice particles drive the radiative balance of clouds, thereby modulating the radiation escaping the planet, their assessment is very important and many studies have shown that the FIR could also be used to improve the sounding of cirrus microphysical properties (e.g., Baran 2007).

Observations of the underexplored FIR spectral region are expected to provide new information on the radiative properties of water vapor and clouds and their role in global warming and to improve our ability to model and assess climate processes, such as forcing and feedback effects.

The first two ground-based experiments developed to cover the FIR spectral region were the Earth Cooling by Water Vapor Radiation (ECOWAR) experiment (Bhawar et al. 2008) that took place in the Italian Alps at 3,500 m MSL in a 2-week period during March 2007 and, nearly simultaneously, the Radiative Heating in Underexplored Bands Campaigns (RHUBC-I) of the U.S. Atmospheric Radiation Measurement (ARM) program at the ARM Climate Research Facility (ACRF) North Slope of Alaska site in Barrow (Turner and Mlawer 2010). A second RHUBC-II campaign took place at Cerro Toco at 5,380 m MSL in the Atacama Desert, Chile, from August to October 2009 (Turner et al. 2012a). All three experiments were mainly focused on performing measurements in clear-sky conditions with the main aim to improve the water vapor spectroscopy in the FIR region. Results from these experiments have helped to refine the spectral characterization of the pure rotational water vapor band with the revision of the continuum absorption coefficients in the FIR between 180 and 600 cm^{-1} (55.6–16.7 μm) (Serio et al. 2008; Delamere et al. 2010; Masiello et al. 2012; Liuzzi et al. 2014). Turner et al. (2012b) demonstrated that the changes made in the water vapor continuum absorption model, after the RHUBC-I and ECOWAR experiments, made a significant impact on both the radiation and dynamics of a global climate model simulation. However, a complete characterization of the FIR component of the atmospheric thermal emission requires measurements in all-sky conditions and for sufficient time to include daily, seasonal, and annual signatures. This can be done from high-altitude ground-based stations characterized by low-humidity values for the whole year, a condition that occurs on the Antarctic Plateau, which is thus an ideal place for a permanent installation of instruments able to perform this kind of measurements.

This paper describes the experiment named Radiative Properties of Water Vapor and Clouds in Antarctica (PRANA; acronym from the Italian project name "Proprietà Radiative dell'Atmosfera e delle Nubi in Antartide") that took place from the high-altitude Antarctic station of Concordia, near the Dome C site, and performed a spectral characterization of the atmospheric downwelling longwave radiance (DLR) from 100 to 1,400 cm^{-1} (100–7.1 μm). This project started in December 2011 and measurements are continuing until the end of 2015 with daily acquisitions systematically performed under different sky conditions. The PRANA experiment supplies the first complete dataset, available through a web interface, of the spectral DLR including the unique measurements in the FIR.

The spectral measurement of the DLR is performed by the Radiation Explorer in the Far Infrared—Prototype for Applications and Development (REFIR-PAD) spectrometer, which was developed in house for field applications from remote sites. To support the spectral measurement, a cloud coverage characterization is performed by using a backscatter and depolarization lidar system. Both instruments have a long record of measurement campaigns: REFIR-PAD was deployed the first time in Brazil with a stratospheric balloon flight in 2005 (Palchetti et al.

2006, 2008a) and then in several ground-based campaigns from high-altitude sites, among which there are ECOWAR and RHUBC-II campaigns cited above, in the 2007–11 period; the lidar system was operated from 2003 to 2006 on board the "Italica" ship in the Ross Sea, and it has been operative at Concordia station since 2007. Both instruments allow full automatic operations over 24 h a day for all the year with remote control from Italy to adjust configuration parameters.

MEASUREMENT SITE AND DEPLOYED INSTRUMENTS. Concordia station is an Antarctic research base located in the Dome C region (75°06'S, 123°23'E) over the Antarctic Plateau at 3,230 m of elevation (Fig. 1). The station was opened in 2005 within an international cooperation project between the Italian National Program for Research in Antarctica (PNRA) and the Institut Polaire Français Paul Émile Victor (IPEV). Concordia station is open all year, hosting about 65 people in summer and 16 people during winter. Experiments conducted in the station span from glaciology to atmospheric physics and astrophysics, and instrumentation is deployed in different installations over an area of 1,500 m^2 around the main buildings (Fig. 2).

The REFIR-PAD spectrometer and the lidar system used in the PRANA project are installed in the "Physics Shelter" (PS), which is located about half a kilometer south of the main station buildings, in the so-called clear area, which is typically windward with respect to the predominant southward winds, minimizing the air contamination due to the exhaust gases coming from the power generator. Measurements are performed through rooftop apertures: Fig. 3 shows a picture from above the shelter rooftop, where the different observation ports are visible. REFIR-PAD looks at the sky through a clear aperture without any window, since in the thermal infrared any material will introduce important absorption/reflection effects that can reduce the calibration accuracy. An insulating material chimney connects internally the instruments to the measurement port protecting the shelter from exposure to the cold air outside. On the rooftop, a wood barrier protects the REFIR-PAD port from winds and snow. The lidar uses two double-glass windows mounted on the rooftop of the shelter. Both windows are kept clean from ice and snow by means of a dry airflow. Figure 3 also shows the location of the line of sight of other instruments installed on the rooftop of the PS that will be briefly introduced in the following section "Other instruments on the site."

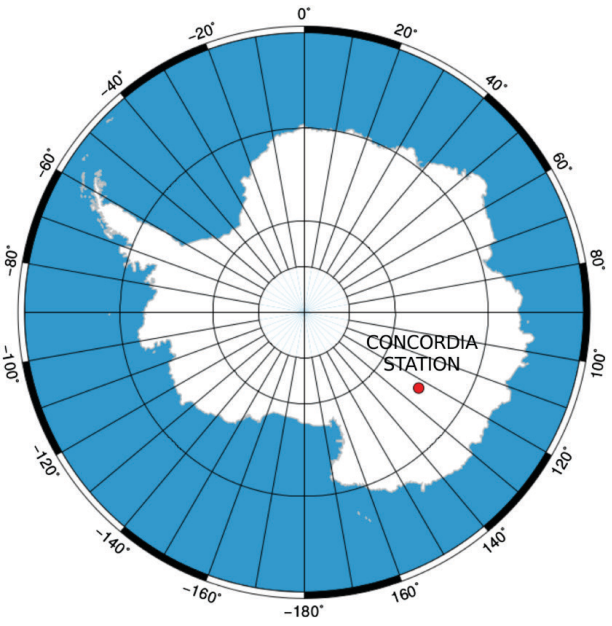

Fig. 1. Location of Concordia station at Dome C over the Antarctic Plateau.

Fig. 2. View of the main buildings of the station. Courtesy of PNRA/IPEV (L. Palchetti).

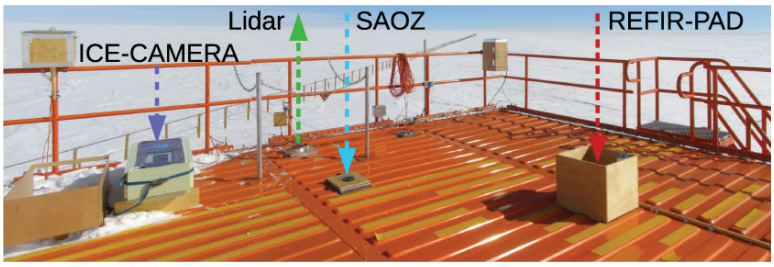

Fig. 3. Line-of-sight location of the main instruments above the Physics Shelter rooftop. Courtesy of PNRA/IPEV (L. Palchetti).

The REFIR-PAD spectrometer. The REFIR-PAD instrument is based on a spectrometer designed for a satellite mission proposed in 1998 in the Fourth European Framework Programme and is called Radiation Explorer in the Far Infrared (Rizzi et al. 2002). REFIR-PAD is the prototype of the main instrument of the REFIR mission and it is a compact and easy to use Fourier transform spectrometer developed both for laboratory and for field applications (Bianchini et al. 2006) with the support of the Italian and European Space Agencies. The spectrometer operates at room temperature using pyroelectric detectors and bilayer amplitude dividing beam splitters that enable good performance over the full thermal infrared.

In the Antarctic deployment, REFIR-PAD operates continuously for 24 h a day with an automatic procedure that controls the acquisition, the preliminary analysis, and the data transmission to Italy. The acquisition is performed in cycles of 9 h with a 66% duty cycle, where 3 h are used for calibrating the spectra (level-1 analysis) that are delivered to the main server in Italy by email. The 9-h cycle was chosen to cover different local times over the year, avoiding systematic biases and thus capturing possible daily signatures.

The REFIR-PAD main specifications during the Antarctic campaign are summarized in Table 1. The instrument covers 100–1,400 cm^{-1} (100–7.1 μm) with a nominal spectral resolution of 0.4 cm^{-1}. The measurement sequence is composed of four calibration acquisitions, in which the instrument looks at the internal reference blackbody sources, and four sky observations. Each single acquisition takes about 80 s and the whole sequence has a duration of about 14 min, including delays for detector settling after scene changes. The REFIR-PAD standard product is the calibrated spectrum of the DLR obtained from a single measurement sequence, averaged on the two detectors and four sky observations (eight spectra total) with associated random and calibration errors. Figure 4 shows some examples of spectra acquired in clear and cloudy sky (top panel), for a cirrus cloud, and for a low-level thick cloud, as well as the typical noise performances (bottom panel) over the full instrumental spectral range.

The measurement of the whole atmospheric thermal emission spectral range allows one to obtain information about the relevant atmospheric components, which contribute to the longwave energy balance. The emitted radiance is modulated by the spectral features of the water vapor (H_20), carbon dioxide (CO_2), ozone (O_3), and clouds, which produce the largest effects. In clear-sky conditions, the measured radiance in the spectral regions where the atmosphere is completely transparent is equal to the emission of the deep space (blue curve in Fig. 4)—that is, negligible. In the other cases, the presence of clouds increases the emission, with a contribution that is visible primarily in the transparent windows, and ranging from the small

Table 1. REFIR-PAD main specifications used in the PRANA experiment.

Parameter	Value
Spectral bandwidth	100–1,400 cm^{-1} (100–7.1 μm)
Spectral resolution	0.4 cm^{-1} (double-sided interferograms)
Optical throughput	0.01 cm^2 sr
Line of sight	Zenith looking with a field of view of about 100 mrad
Single-spectrum integration time	80 s
Measurement time	6.5 min (average of four observations), every 14 min (sequence duration)
NESR	About 10^{-3} W m^{-2} cm sr^{-1} at 400 cm^{-1} (25 μm)
Instrument mass	55 kg
Instrument size	62 cm × 50 cm × 26 cm
Power supply	50 W (average), 70 W (peak)

effect of a thin cirrus cloud (red curve in Fig. 4) to the strong emission of a completely opaque atmosphere typical of low clouds (black curve in Fig. 4). As shown in Fig. 4, all the atmospheric spectral features are well resolved by the REFIR-PAD measurements. The positive signal peaks above the blackbody curve corresponding to the thick clouds are a local effect due to the emission of the first part of the measurement path, which is inside the protected chimney, just above the instrument, and therefore at higher temperature than outside (chimney effect).

Measurement error is estimated for each average spectrum, following the approach outlined in Bianchini and Palchetti (2008), by calculating the radiometric noise equivalent spectral radiance (NESR) due to detector noise, the calibration error (Cal Err) due to the calibration uncertainty, and the standard deviation of the mean (STD). STD is an a posteriori estimation, which includes the instrument NESR (cited above) and also takes into account possible scene variations that can be present during the acquisition in cloudy conditions. As shown in the figure, the noise components are typically between 0.001 and 0.002 W m^{-2} cm sr^{-1} and increase in the strong absorption lines of pure rotational H_2O band below 600 cm^{-1} (above 16.7 μm) and CO_2 band around 667 cm^{-1} (15 μm) as a result of gases inside the instrument path that reduce its efficiency. The strong absorption bands of the polyethylene terephthalate (PET) substrate, with which the wideband beam splitters are made, also reduce the instrument efficiency. In particular, the PET absorption intervals of 1,095–1,140 and 1,230–1,285 cm^{-1} (9.13–8.77 and 8.13–7.78 μm, respectively) have been removed from the plotted spectra because of the high value of the measured noise.

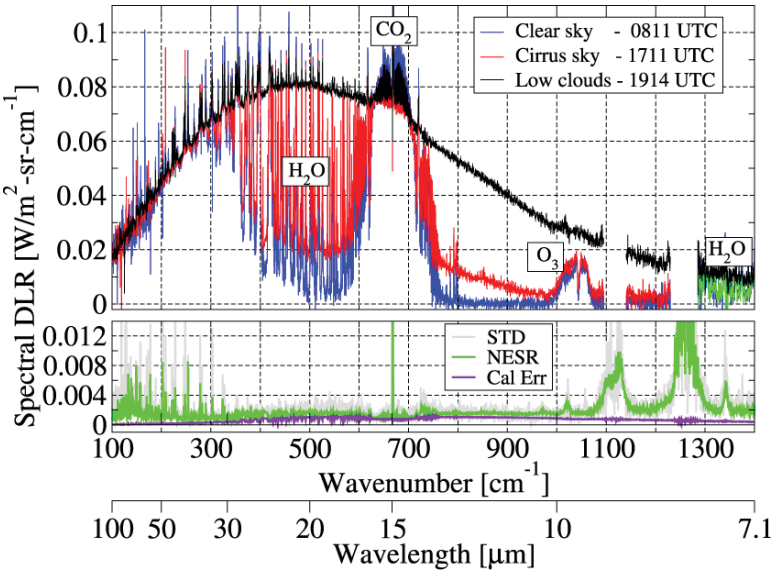

Fig. 4. (top) Wideband spectra taken under different sky conditions and (bottom) typical noise performance measured on 2 Jan 2013.

Lidar system. The lidar is a backscatter and depolarization system currently operating at Concordia station in the framework of different projects (http://lidarmax.altervista.org/englidar/_Antarctic%20LIDAR.php). It allows the continuous measurement of vertical profiles of aerosol and the cloud structure and the determination of the physical phase of particles. Daily plots in false colors, obtained with an automatic procedure, are delivered to Italy to monitor the scene and for checking instrument operations. The main specifications that characterize the lidar are shown in Table 2.

Weather station. The ground atmospheric conditions are supplied by a weather station (Vaisala WXT520) installed on the rooftop of the PS at a few meters from the REFIR-PAD view aperture. The station is configured to supply the measurement of six weather parameters: wind speed and direction, precipitation, atmospheric pressure P, temperature T, and relative humidity U every 10 s. These ancillary parameters can be used to constrain the ground atmospheric layer seen by the spectrometer.

Other instruments on the site. As far as atmospheric studies are concerned, Concordia station hosts many projects, which routinely supply a large set of atmospheric parameters. Here we summarize the

Table 2. Lidar system main specifications used in the Antarctic measurements.

Parameter	Value
Channels	Backscatter and depolarization channels
Wavelength	532 nm (linear polarization)
Measurement range	30–7,000 m AGL
Vertical resolution	7.5-m resolution
Line of sight	Zenith looking through a window all weather
Telescope	10-cm diameter, f = 30-cm refractive optics
Filter	0.15-nm interference filter
Laser	Quantel (Brio)

Table 3. Other instruments deployed at Concordia station for different projects. PS indicates the Physics Shelter, where REFIR-PAD is installed.

Instrument	Reference	Location	Key features
Routine meteorological observations: radiosondes	IPEV/PNRA	Main buildings at 500 m from PS	*P*, *T*, *U*, and wind; daily vertical profiles at 1200 UTC
Baseline Surface Radiation Network (BSRN)	Dr. V. Vitale, ISAC-CNR, Italy	100 m from PS	Downwelling and upwelling shortwave and longwave radiation
H_2O Antarctica Microwave Stratospheric and Tropospheric Radiometers (HAMSTRAD)	Dr. P. Ricaud, Météo-France, GAME/CNRS, Toulouse, France	PS	Tropospheric vertical profiles of water vapor and temperature
Système d'Analyze par Observation Zénithale (SAOZ)	Dr. J.-P. Pommereau, LATMOS–IPSL, France	PS	Total O_3 and NO_2; vertical columns from UV–visible spectrometer
Ice scan camera (ICE-CAMERA)	Dr. M. Del Guasta, INO-CNR, Italy	PS	Crystal shape images

instruments and the available datasets (see Table 3) that can add complementary or synergistic information to exploit the scientific objectives of the PRANA project.

Radio soundings (RS) observations are performed daily at 1200 UTC by IPEV/PNRA within the project "Routine Meteorological Observation at Station Concordia" (www.climantartide.it/index.php?lang=en). The measurements include the vertical profiles of pressure, temperature, humidity, and wind speed and direction from ground to the altitude of 25–30 km, typically. These measurements can be used to supply ancillary information on the atmospheric state and to validate the profiles retrieved from the REFIR-PAD spectra (see section "Initial results"). Given the importance of using this information to better exploit REFIR-PAD observations, the RS profiles are made available together with the REFIR-PAD dataset.

A series of standard radiometers, located at about 100 m from REFIR-PAD, measure the downwelling and upwelling radiation, in both the shortwave and the longwave ranges, within the Baseline Surface Radiation Network (BSRN) of the World Climate Research Programme. These measurements give information about the radiation budget at ground level and are available since 2006 for the downwelling component and since 2007 for the upwelling component (Lanconelli et al. 2011) (http://bsrn.awi.de). The interest for these measurements is related to the possibility of performing a comparison between the BSRN longwave downwelling measurement and the analogous quantity derived from the spectrally resolved observation performed by REFIR-PAD. This comparison will allow the identification of the contribution of the different species, by means of the spectral measurements, on the surface radiation budget.

The H_2O Antarctica Microwave Stratospheric and Tropospheric Radiometers (HAMSTRAD), deployed in 2009, is a microwave radiometer (two bands at 60 and 183 GHz) that supplies vertical profiles of water vapor and temperature every 7 min, from 0 to about 10 km above ground level with a vertical resolution from about 30 to 50 m in the planetary boundary layer, and about 500 m in the upper troposphere–lower stratosphere with the aim to study possible trends (Ricaud et al. 2013) (www.cnrm-game-meteo.fr/?lang=en). The measured profiles can be used to perform a cross check with the analogous products derived by the REFIR-PAD measurements.

The Système d'Analyze par Observation Zénithale (SAOZ) is operative at Dome C since 2007 and supplies ozone and nitrogen dioxide columns in daytime (Pommereau and Goutail 1988) (http://saoz.obs.uvsq.fr/). For the PRANA project, the ozone measurement can be useful to constrain the species concentration in the analysis of the REFIR-PAD spectra.

Finally, the ice scan camera (ICE-CAMERA), installed in 2012, is an image scanner modified to capture high-resolution images of the shape of ice crystals, which precipitate over the instrument (http://lidarmax.altervista.org/lidar/_Precipitazioni%20in%20Antartide.php). The ICE-CAMERA instrument gives an automatic classification of the precipitation that can be used to identify possible spectral signature in the REFIR-PAD thermal infrared spectrum of the precipitating particles.

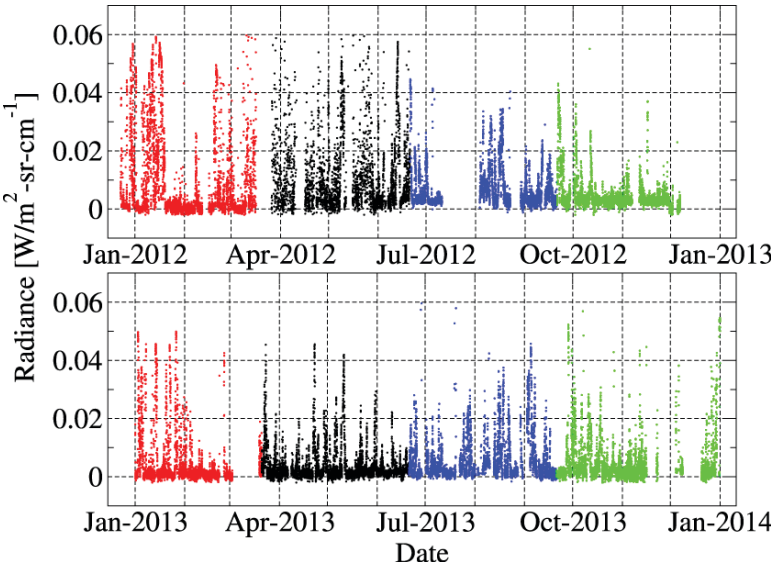

Fig. 5. Mean radiance in the 828–839-cm^{-1} (12.077–11.919 μm) spectral channels over 2 years, during the Antarctic spring (green), summer (red), fall (black), and winter (blue). Missing points are due to power supply failure.

INITIAL RESULTS. During the 2 years of the PRANA project, REFIR-PAD was operated almost continuously every day. Only a few interruptions occurred as a result of the failure of the main power supply of the shelter or for the instrument maintenance during the summer campaigns in December. The most important loss of measurements of a few days occurred in March and July 2012 and March 2013.

To give an estimation of the absolute accuracy of the measurements, an average of the radiance measured in the atmospheric window, in the spectral channels between 828 and 839 cm^{-1} (12.077–11.919 μm), is calculated for each measurement for the whole dataset. In this narrow spectral region, the atmosphere is completely transparent since no emission line is present; therefore, in clear-sky conditions the measured radiance is equal to zero, corresponding to the nearly zero emission of the deep space. In cloudy conditions, the measured radiance is due to the emission of clouds and is substantially different from zero.

The plot of the average radiance in the 828–839-cm^{-1} channels, shown in Fig. 5, is therefore an estimation of the sky cloudiness and, in the case of clear sky, an estimation of the absolute calibration error of the measurement. Since most of the observations are in clear sky and most of the measurements have a signal in the 828–839-cm^{-1} channels below 0.0015 W m^{-2} cm sr^{-1}, to find an estimation of the calibration error, only spectra having the 828–839-cm^{-1} radiance below this value have been considered. This condition could select not only the clear-sky cases but also some cases with very thin clouds. However, the frequency of very thin clouds is very low, and the average radiance in the 828–839-cm^{-1} channels can be considered a good estimation of the calibration error, even with a small overestimation. The plot of the monthly averages of this quantity is shown in black in Fig. 6 with the error bars corresponding to the standard deviation of the mean. The curve shows that a small bias over the 2-yr measurements of about 0.0005 W (m^2 sr cm^{-1})$^{-1}$ corresponding to 0.5 K for a blackbody at 240 K is present. This value obtained in

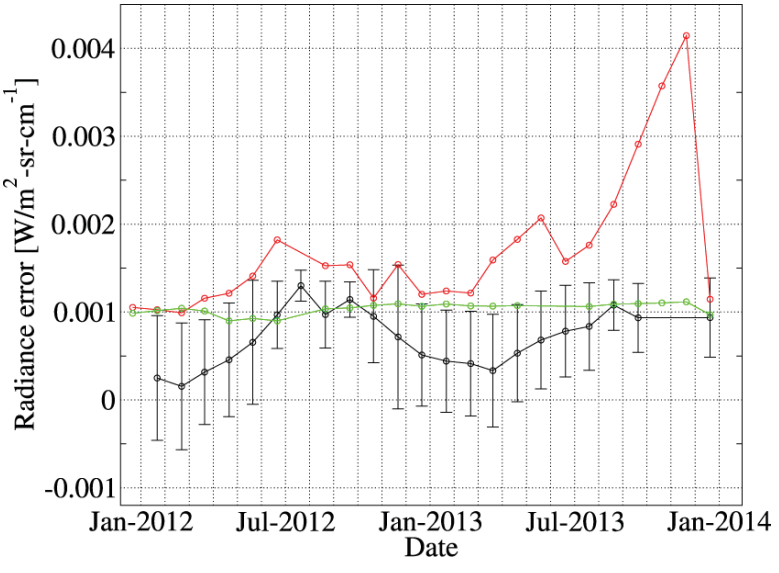

Fig. 6. Monthly averages of the absolute radiance error with standard errors (black curves) measured in the 828–839-cm^{-1} spectral channels for the 2-yr dataset. The corresponding mean values of NESR (red curve) and Cal Err (green curve) of a single measurement are also shown for comparison.

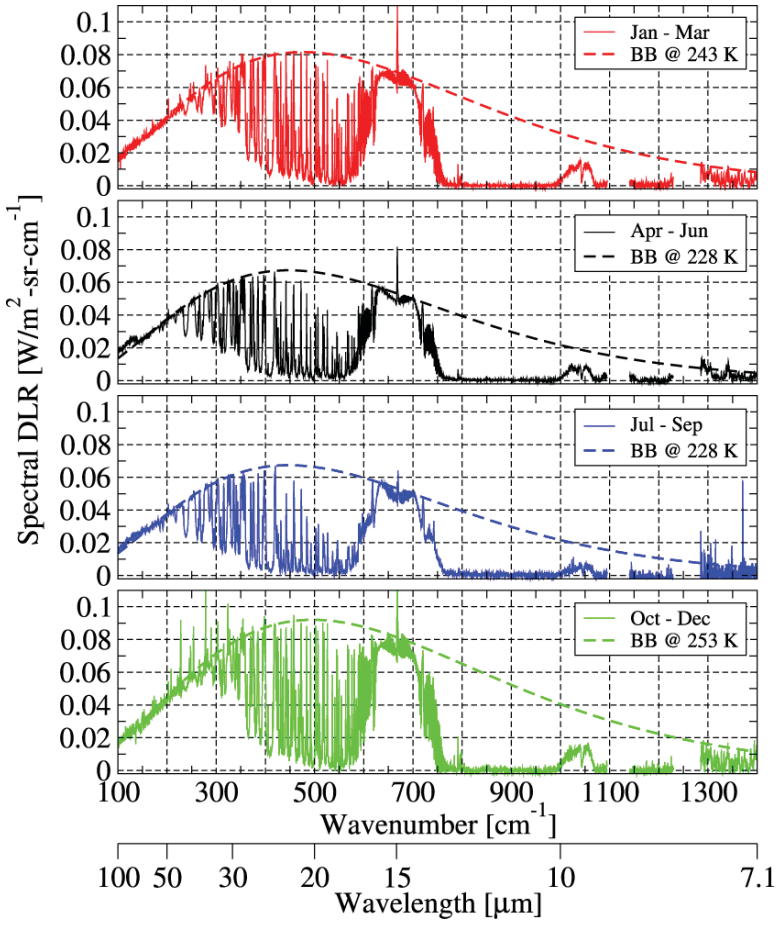

Fig. 7. Seasonal averages of the DLR spectrum (solid lines) during the Antarctic summer (red), fall (black), winter (blue), and spring (green) 2012, compared with the blackbody emission curves (dashed lines) at the temperatures of the air near the instrument.

the 828–839-cm^{-1} spectral channels can be considered a good estimate also for the other spectral regions, since the main source of the calibration error is the uncertainty with which the temperature of the reference blackbodies is known (Palchetti et al. 2008b). We notice that the accuracy is higher in the summertime after the annual maintenance (December–January) operations in which the alignment is optimized and the optics are cleaned. This effect is more evident in the estimation of Cal Err of each single measurement, monthly averaged in the red curve of Fig. 6, which is an a priori estimation of the single measurement accuracy based on the effective instrument efficiency and therefore strongly dependent on misalignment and quality of the optics in particular at 828–839 cm^{-1}.

Figure 7 shows the seasonal averages (3-month average) of spectra acquired with the in clear-sky conditions during 2012. In the spectral regions where the atmosphere is opaque—that is, in the CO_2 band around 667 cm^{-1} (15 μm) and the H_2O band below 400 cm^{-1} (25 μm)—the radiance is higher, since it primarily comes from emission in the lowest few layers of the atmosphere near the surface and follows the typical emission curve of a blackbody at a temperature near the instrument, as shown, in the case of spring time, by the green curves of Fig. 7. In fall and wintertime, when the vertical temperature structure has a strong inversion layer (up to 25 K) near the surface, which is typical of the Antarctic atmosphere, the measured spectrum shows a dip around the central peak of the CO_2 band due to the colder lower levels. The black (fall) and blue (winter) curves in Fig. 7 show the occurrence of this effect. Another detail revealed by the seasonal averages is the higher transparency in the FIR region that allows us to observe spectral features in the pure rotational water vapor band down to 180 cm^{-1} (55.6 μm) in wintertime when the precipitable water vapor is as low as 0.1 mm.

A 2-yr map of the clear-sky spectra converted in brightness temperature (BT) is shown in Fig. 8. The map shows temperature increases during the summertime at the wavenumber where the emission of H_2O, CO_2, and 0_3 are located. The figure also shows that for many days in winter, between May and September, the BT in the FIR is very low owing to the high transparency of the atmospheric windows. The high number of transparency windows from 230 to 1,200 cm^{-1} (43.5–8.3 μm) allows not only improvement of the characterization of the rotational water vapor band (Liuzzi et al. 2014) but also extension of the characterization of the radiative effects of clouds to the FIR region. In this region some models exist (Yang et al. 2013), but only a few measurements were performed from the ground because of the high opacity of the atmosphere due to the water vapor absorption. Finally, Fig. 8 also shows a very interesting difference in the downwelling radiance observed in the ozone band at 1,043 cm^{-1} (9.6 μm) during the two winters, with the data near September 2012 showing a lower signal than in the same months in 2013. Indeed, in 2012 the Antarctic ozone hole was larger than in 2013 and extended over the site of

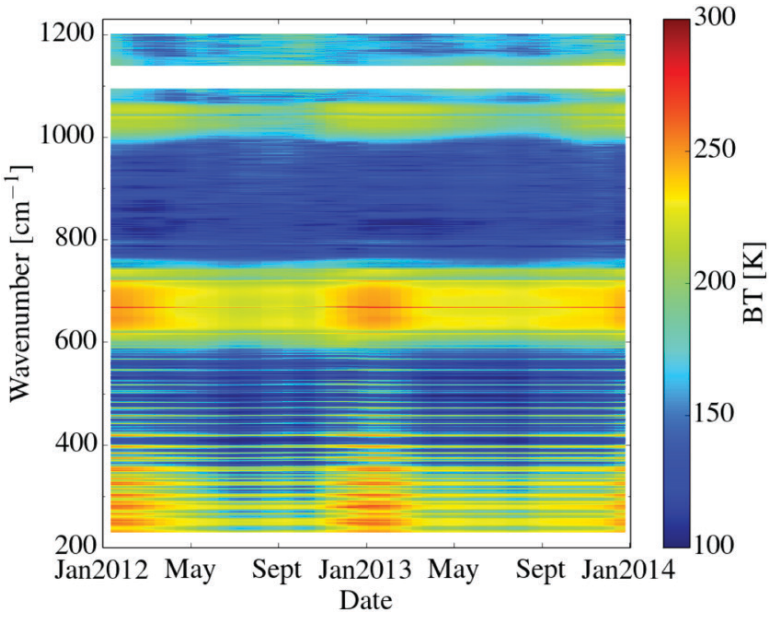

Fig. 8. Map of the spectral brightness temperatures from 230 to 1,200 cm^{-1} (43.5–8.3 μm) in clear sky over 2-yr measurements.

Concordia station almost every day. Actually the radiance depends not only on the ozone concentration but also on the stratospheric temperature, which must be provided by independent measurements to perform a retrieval of the ozone concentration. However, this example shows how spectrally resolved measurements of the DLR could also be useful to study stratospheric processes within the Antarctic polar vortex, such as the ozone chemistry and its relation with the polar stratospheric clouds, all over the year, complementing the standard measurements performed by UV radiometry that are possible only during the period of solar illumination.

The main atmospheric parameters that have an effect in the measured spectral range—that is, H_2O and temperature (through CO_2) profiles, ozone columnar amount, and cloud microphysics—can be retrieved by fitting the measurement against the radiance provided by a radiative transfer model. As an example, REFIR-PAD measurements were used to retrieve vertical profiles of H_2O and temperature by fitting the measurement in the 230–980-cm^{-1} (43.5–10.2 μm) spectral range with the Line-By-Line Radiative Transfer Model (LBLRTM, v12.2; Clough et al. 2005) in clear-sky conditions. The calculation is performed by minimizing the difference between the measurement and the simulation using the least squares method (Bianchini et al. 2011). The measurement does not allow high vertical sensitivity; only a few independent levels can be retrieved. The simulation was performed using 37 atmospheric levels, but only 5 independent levels for H_2O and 4 for the temperature (including 1 level for describing the local chimney effect due to the 2-m-long path propagation through the observation chimney inside the shelter) were fitted. Figure 9 shows the fit results for a measurement performed in wintertime on 27 June 2013. The residual difference between measurement and model (green curve) is always within the noise estimation (black curves) with $\chi^2 = 0.75$. The fitted vertical profiles of H_2O and temperature, obtained for this case, are shown in Fig. 10, where they are compared with the climatological profiles used as initial guesses to initialize the fit procedure and the radiosonde profiles measured at the same time. While the fitting procedure provides profiles throughout the troposphere, the observations are most sensitive to the lower-atmospheric structure in both water

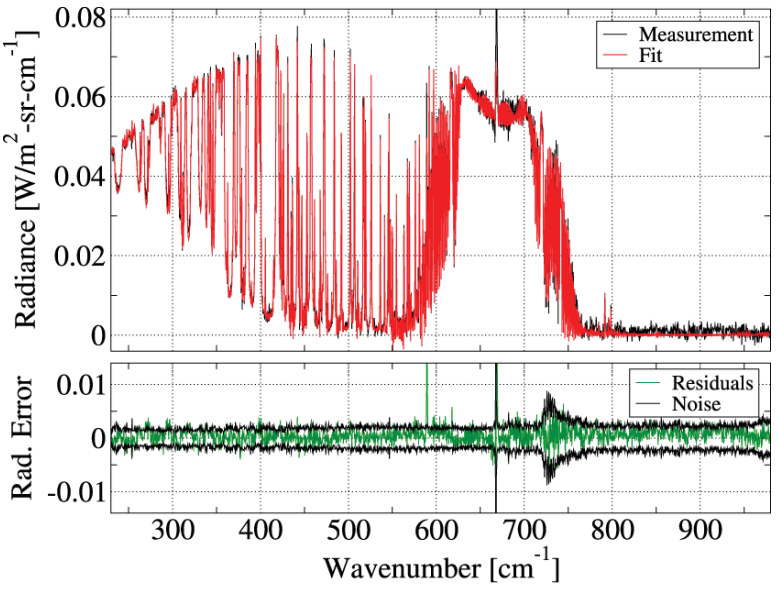

Fig. 9. (top) Measured and fitted spectra for the REFIR-PAD observation at 1152 UTC 27 Jun 2013 and (bottom) the residual difference compared with the measurement noise.

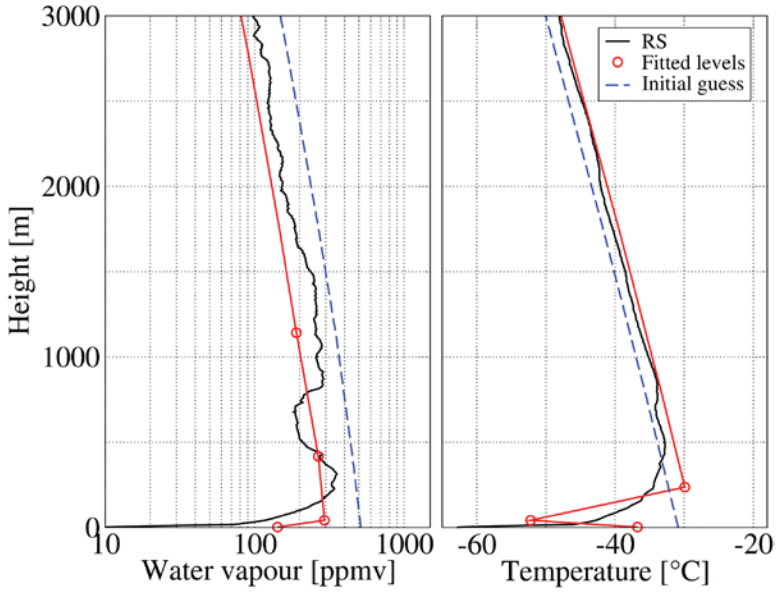

Fig. 10. Comparison between the RS and the fitted vertical profiles for (left) the water vapor and (right) the temperature obtained for the spectrum in Fig. 9. The initial-guess profiles used in the fit procedure are also shown.

vapor and temperature. The retrieval profiles are also strongly affected by the warmer and more humid area above the shelter and inside the observation chimney. The presence of this layer, characterized by extremely different conditions with respect to the outside, especially in the wintertime, complicates the geometry structure chosen for the fitting. Nevertheless, the comparison with radiosonde measurements, shown in Fig. 10, where the lower-layer values due to the chimney effect were not plotted, demonstrate the capability to take the main features of the vertical profiles, even taking into account the low vertical resolution.

As a case study in cloudy-sky conditions, the measurements performed on 6 October 2013 are considered. The lidar maps in Fig. 11 show the presence of different cloud structures during the day: a precipitating ice cloud early in the morning and high cirrus in the afternoon starting to precipitate around 1900 UTC. A similar picture can be observed in the spectral BT map in Fig. 12, where the presence of cloud is identified by the increasing BT in the transparent windows, in particular above 750 cm^{-1} (13.3 μm). It should be noted that REFIR-PAD measures only 6 out of 9 h and therefore the measurements are discontinuous. Here we analyze the measurement at 1817 UTC, identified in Fig. 11 by a black vertical line, by performing a fit with a simultaneous determination of the atmospheric vertical water vapor and temperature profiles and the cirrus microphysics. The radiative transfer uses LBLRTM to model the effect of the atmospheric status (as described above for the water vapor and temperature profiles) and the available scattering and absorption property databases to model the properties of cirrus clouds covering the extended spectral range of REFIR-PAD. In particular, for ice particles, we use the semiempirical model developed by Fu et al. (1998) and, for water droplets, we use the database supplied by Hu and Stamnes (1993). In this way the cloud microphysics are retrieved as the effective particle diameter, the ice water path, the fractional ice content with respect to liquid water, and the effective cloud temperature. In the model, the cirrus is approximated by a single uniform layer with

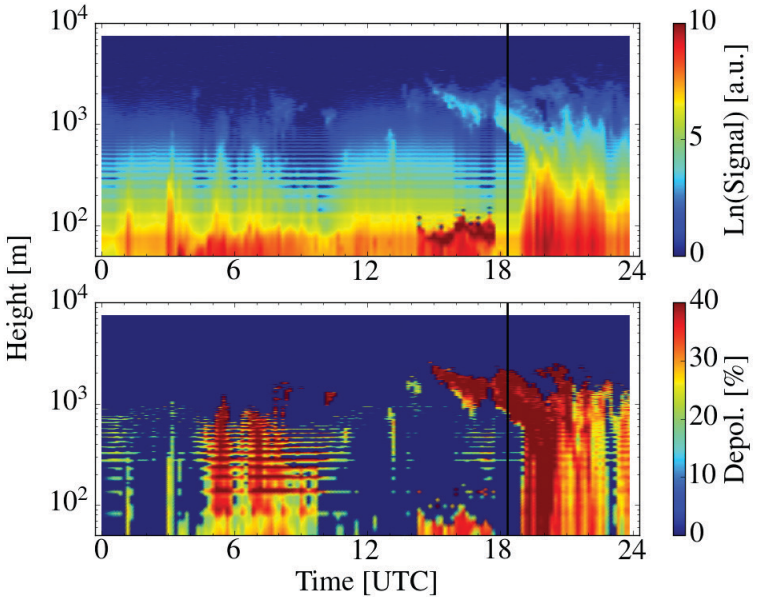

Fig. 11. (top) Lidar backscatter and (bottom) depolarization ratio measured on 6 Oct 2013. The black vertical line identifies the REFIR-PAD measurement at 1817 UTC used for the fitting. The "temporal horizontal stripes" are a spurious effect due to a bad electrical contact among signal cables, which hit the acquisition in 2013.

the thickness given by the lidar measurement and the temperature given by the effective value calculated by weighting the vertical temperature profile with the lidar backscatter cloud profile (left and center panels of Fig. 13). In this way, the cloud effective temperature is closely related in the fitting procedure to the retrieved atmospheric vertical temperature profile. The fit for the analyzed case gives an effective cloud temperature of –37.8°C, an ice effective diameter of 20 μm, a total water path of 9 g m^{-2}, and an ice fraction of 84%. The corresponding optical depth turns out to be 1.5. Even though these parameters cannot be completely validated for the lack of direct measurements of the cloud microphysics, nevertheless the approach of using the spectrally resolved full-spectral-band thermal emission measurements shows the feasibility of performing the remote sensing of cloud parameters, provided that a validated cloud model is supplied. As far as the fitting of the atmospheric state is concerned, the resulting vertical profiles are compared in center and right panels of Fig. 13 for validation with the collocated radiosonde measurements performed at 1200 UTC. The comparison shows a good agreement considering that the radiosonde was launched a few hours before and that the larger discrepancies in the lower layers are due to the known local warming effects of the first layer inside the shelter.

AVAILABLE DATASET. The 2-yr acquisitions dataset provided by the PRANA project is composed by the REFIR-PAD calibrated spectra of the DLR, the Physics Shelter weather station, the lidar backscatter and depolarization ratio measurements, and the RS vertical profiles. The list of the available measurements with acquisition time information is shown in Table 4. The REFIR-PAD, weather station data, and RS data are supplied in ASCII format with UTC timestamp, whereas the lidar parameters are supplied in daily color maps, as in Fig. 11.

The dataset is being made publicly available at the REFIR website (http://refir.fi.ino.it) for the emission spectra, the weather parameters, and the RS profiles and online (http://lidarmax.altervista.org/englidar/_Antarctic%20LIDAR.php) for the lidar maps. The access to spectral, weather, and RS data requires permission, which will be granted to everyone who is interested in working on these data.

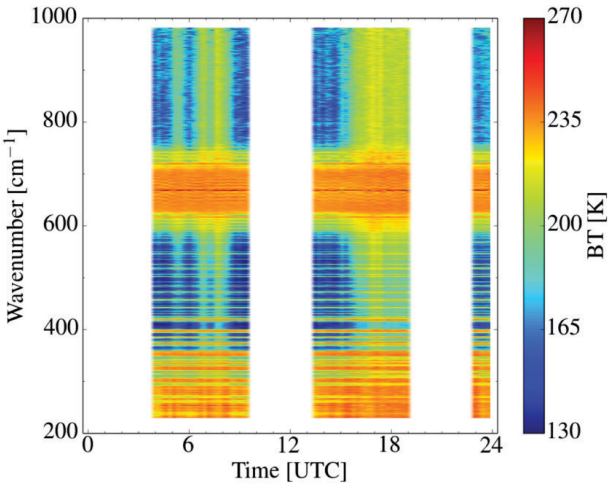

FIG. 12. REFIR-PAD spectral brightness temperature (right ordinate) plotted for the fitting spectral interval 230–980 cm^{-1} (43.5–10.2 μm; left ordinate) measured on 6 Oct 2013. The instrument takes atmospheric measurements for 6 out of 9 h. For the remaining 3 h, data analysis is performed and observations are not available (white bars in the plot).

CONCLUSIONS. We present a unique dataset of spectral measurements in the thermal infrared, which covers the longwave region of the downwelling atmospheric emission with systematic acquisitions taken almost continuously for 2 years from the Antarctic site of the Concordia station at Dome C. Thanks to the extremely low temperature and humidity of this site, the acquired spectra have sufficient transparency to cover all the relevant spectral range of the longwave thermal emission from the FIR at 100 cm^{-1} (100 μm) up to the middle IR at 1,400 cm^{-1} (7.1 μm).

This spectral range contains the signatures of the main absorbers of the atmosphere: water vapor,

TABLE 4. 2012/13 PRANA dataset.

Instrument	Measured quantity	Time resolution	Operating time
REFIR-PAD	Downwelling spectral radiances	14 min	6 of 9 h
Lidar	Vertical backscatter profiles	10 min	24 of 24 h
Lidar	Vertical depolarization ratio profiles	10 min	24 of 24 h
Ground weather station	Ground *P*, *T*, and *U*	10 s	24 of 24 h
Radio sounding	*P*, *T*, *U*, and wind vertical profiles (from the ground to 25–30 km)	1 day	1200 UTC

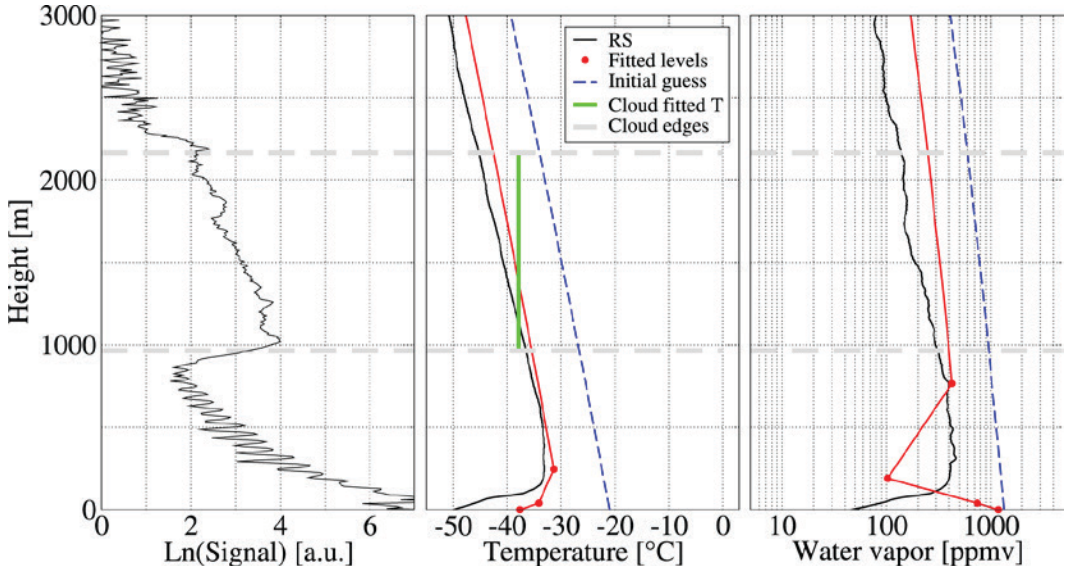

Fig. 13. (left) Lidar backscatter profile and (center) temperature and (right) water vapor fitted profiles compared with RS and initial guess profiles for the observation performed at 1817 UTC 6 Oct 2013. The center panel also shows the fitted cloud effective temperature T = −37.8°C (green).

carbon dioxide, and cirrus clouds from the troposphere and ozone and PSC from the stratosphere. The measurement therefore provides radiative information about all these components and the radiative coupling among the different layers of the atmosphere from the surface up to the stratosphere. The coverage of the FIR range, for the first time over the very dry Antarctic Plateau and under different seasons and atmospheric conditions, can improve greatly our knowledge of the radiative properties of these components in the longest wave range of the emission.

We qualify the measurement by calculating the calibration error, measured for the whole dataset—that is, of about 0.5 K in brightness temperature with respect to the emission of a blackbody at 240 K. We also show how this kind of measurement can be used for the remote sensing of the atmospheric state by retrieving both the vertical profiles of water vapor and temperature and the cloud microphysics. The obtained atmospheric profiles are also compared, both in clear-sky and cloudy conditions, with measurements performed by the collocated radiosounding, showing a general good agreement among measurements.

Finally, after the PRANA project ended in May 2014, REFIR-PAD continues to be operated and supplies the same kind of measurements in the framework of a new project named Concordia Multi-Process Atmospheric Studies (CoMPASs), which was designed to study the vertical structure of the Antarctic atmosphere with a synergy of different remote sensing techniques. Within new projects, the REFIR-PAD spectral dataset will be continuosly expanded with other measurements. Currently the acquired spectra are shown every day after a preliminary analysis online (http://refir.fi.ino.it/rtDomeC).

It is expected that a better characterization of the FIR spectrum of water vapor and thin clouds, such as cirrus and polar stratospheric clouds, and ozone performed with this measurement covering many years and different weather conditions, will contribute to improve the accuracy of climate model previsions.

ACKNOWLEDGMENTS. This research was supported by the Italian PNRA (Programma Nazionale di Ricerche in Antartide) and the Institut polaire français Paul Émile Victor (IPEV). More specifically it was developed as a part of the Subproject PRANA (Proprietà Radiative dell'Atmosfera e delle Nubi in Antartide). Data and information on radio sounding measurements were obtained from the IPEV/PNRA Project "Routine Meteorological Observation at Station Concordia" (www.climantartide.it/index.php?lang=en). We thank all of the institutions and their associates listed in Table 3 for supplying information about other measurements available at Concordia station.

REFERENCES

Baran, A. J., 2007: The impact of cirrus microphysical and macrophysical properties on upwelling far-infrared spectra. *Quart. J. Roy. Meteor. Soc.*, **133,** 1425–1437, doi:10.1002/qj.132.

Bhawar, R., and Coauthors, 2008: Spectrally resolved observations of atmospheric emitted radiance in the H_2O rotation band. *Geophys. Res. Lett.,* **35,** L04812, doi:10.1029/2007GL032207.

Bianchini, G., and L. Palchetti, 2008: Technical note: REFIR-PAD level 1 data analysis and performance characterization. *Atmos. Chem. Phys.,* **8,** 3817–3826, doi:10.5194/acp-8-3817-2008.

——, ——, and B. Carli, 2006: A wide-band nadir-sounding spectroradiometer for the characterization of the Earth's outgoing long-wave radiation. *Sensors, Systems, and Next-Generation Satellites X,* R. Meynart, S. P. Neeck, and H. Shimoda, Eds., International Society for Optical Engineering (SPIE Proceedings, Vol. 6361), doi:10.1117/12.689260.

——, ——, G. Muscari, I. Fiorucci, P. Di Girolamo, and T. Di Iorio, 2011: Water vapor sounding with the far infrared REFIR-PAD spectroradiometer from a high-altitude ground-based station during the ECOWAR campaign. *J. Geophys. Res.,* **116,** D02310, doi:10.1029/2010JD014530.

Clough, S. A., M. J. Iacono, and J.-L. Moncet, 1992: Line-by-line calculations of atmospheric fluxes and cooling rates: Application to water vapor. *J. Geophys. Res.,* **97,** 15 761–15 785, doi:10.1029/92JD01419.

——, M. W. Shephard, E. J. Mlawer, J. S. Delamere, M. J. Iacono, K. Cady-Pereira, S. Boukabara, and P. D. Brown, 2005: Atmospheric radiative transfer modeling: A summary of the AER codes. *J. Quant. Spectrosc. Radiat. Transfer,* **91,** 233–244, doi:10.1016/j.jqsrt.2004.05.058.

Conrath, B. J., R. A. Hanel, V. G. Kunde, and C. Prabhakara, 1970: The infrared interferometer experiment on Nimbus 3. *J. Geophys. Res.,* **75,** 5831–5857, doi:10.1029/JC075i030p05831.

Delamere, J. S., S. A. Clough, V. H. Payne, E. J. Mlawer, D. D. Turner, and R. R. Gamache, 2010: A far-infrared radiative closure study in the Arctic: Application to water vapor. *J. Geophys. Res.,* **115,** D17106, doi:10.1029/2009JD012968.

Fu, Q., P. Yang, and W. B. Sun, 1998: An accurate parameterization of the infrared radiative properties of cirrus clouds for climate models. *J. Climate,* **11,** 2223–2237, doi:10.1175/1520-0442(1998)011<2223:AAPOTI>2.0.CO;2.

Harries, J., and Coauthors, 2008: The far-infrared Earth. *Rev. Geophys.,* **46,** RG4004, doi:10.1029/2007RG000233.

Hu, Y. X., and K. Stamnes, 1993: An accurate parameterization of the radiative properties of water clouds suitable for use in climate models. *J. Climate,* **6,** 728–742, doi:10.1175/1520-0442(1993)006<0728:AAPOTR>2.0.CO;2.

Lanconelli, C., M. Busetto, E. Dutton, G. König-Langlo, M. Maturilli, R. Sieger, V. Vitale, and T. Yamanouchi, 2011: Polar baseline surface radiation measurements during the International Polar Year 2007–2009. *Earth Syst. Sci. Data,* **3,** 1–8, doi:10.5194/essd-3-1-2011.

Liuzzi, G., G. Masiello, C. Serio, L. Palchetti, and G. Bianchini, 2014: Validation of H_2O continuum absorption models in the wave number range 180-600 cm^{-1} with atmospheric emitted spectral radiance measured at the Antarctica Dome-C site. *Opt. Express,* **22,** 16 784–16 801, doi:10.1364/OE.22.016784.

Masiello, G., C. Serio, F. Esposito, and L. Palchetti, 2012: Validation of line and continuum spectroscopic parameters with measurements of atmospheric emitted spectral radiance from far to mid infrared wave number range. *J. Quant. Spectrosc. Radiat. Transfer,* **113,** 1286–1299, doi:10.1016/j.jqsrt.2012.01.019.

Mlynczak, M. G., and Coauthors, 2002: Far-infrared: A frontier in remote sensing of Earth's climate and energy balance. *Optical Spectroscopic Techniques, Remote Sensing, and Instrumentation for Atmospheric and Space Research IV,* A. M. Larar and M. G. Mlynczak, Eds., International Society for Optical Engineering (SPIE Proceedings, Vol. 4485), doi:10.1117/12.454247.

——, D. G. Johnson, G. E. Bingham, K. W. Jucks, W. A. Traub, L. Gordley, and P. Yang, 2006a: The far-infrared spectroscopy of the troposphere (FIRST) project. *Enabling Sensor and Platform Technologies for Spaceborne Remote Sensing,* G. J. Komar, J. Wang, and T. Kimura, Eds., International Society for Optical Engineering (SPIE Proceedings, Vol. 5659), doi:10.1117/12.579063.

——, and Coauthors, 2006b: First light from the far-infrared spectroscopy of the troposphere (FIRST) instrument. *Geophys. Res. Lett.,* **33,** L07704, doi:10.1029/2005GL025114.

Palchetti, L., and Coauthors, 2006: Technical note: First spectral measurement of the Earth's upwelling emission using an uncooled wideband Fourier transform spectrometer. *Atmos. Chem. Phys.,* **6,** 5025–5030, doi:10.5194/acp-6-5025-2006.

——, G. Bianchini, B. Carli, U. Cortesi, and S. Del Bianco, 2008a: Measurement of the water vapour vertical profile and of the Earth's outgoing far infrared flux. *Atmos. Chem. Phys.,* **8,** 2885–2894, doi:10.5194/acp-8-2885-2008.

——, ——, and F. Castagnoli, 2008b: Design and characterisation of black-body sources for infrared wide-band Fourier transform spectroscopy. *Infrared Phys. Technol.,* **51,** 207–215, doi:10.1016/j.infrared.2007.06.001.

Pommereau, J. P., and F. Goutail, 1988: Stratospheric O_3 and NO_2 observations at the southern polar circle

in summer and fall 1988. *Geophys. Res. Lett.,* **15,** 895–897, doi:10.1029/GL015i008p00895.

Ricaud, P., and Coauthors, 2013: Quality assessment of the first measurements of tropospheric water vapor and temperature by the HAMSTRAD Radiometer over Concordia Station, Antarctica. *IEEE Trans. Geosci. Remote Sens.,* **51,** 3217–3239, doi:10.1109/TGRS.2012.2225627.

Rizzi, R., and Coauthors, 2002: Feasibility of the space-borne radiation explorer in the far infrared (REFIR). *Optical Spectroscopic Techniques, Remote Sensing, and Instrumentation for Atmospheric and Space Research IV,* A. M. Larar and M. G. Mlynczak, Eds., International Society for Optical Engineering (SPIE Proceedings, Vol. 4485), doi:10.1117/12.454252.

Serio, C., and Coauthors, 2008: Retrieval of foreign-broadened water vapor continuum coefficients from emitted spectral radiance in the H_2O rotational band from 240 to 590 cm^{-1}. *Opt. Express,* **16,** 15 816–15 833, doi:10.1364/OE.16.015816.

Stocker, T. F., and Coauthors, Eds., 2014: *Climate Change 2013: The Physical Science Basis.* Cambridge University Press, 1535 pp, doi:10.1017/CBO9781107415324.

Turner, D. D., and E. J. Mlawer, 2010: The radiative heating in underexplored bands campaigns. *Bull. Amer. Meteor. Soc.,* **91,** 911–923, doi:10.1175/2010BAMS2904.1.

——, and Coauthors, 2012a: Ground-based high spectral resolution observations of the entire terrestrial spectrum under extremely dry conditions. *Geophys. Res. Lett.,* **39,** L10801, doi:10.1029/2012GL051542.

——, A. Merrelli, D. Vimont, and E. J. Mlawer, 2012b: Impact of modifying the longwave water vapor continuum absorption model on community Earth system model simulations. *J. Geophys. Res.,* **117,** D04106, doi:10.1029/2011JD016440.

Yang, P., and Coauthors, 2003: Spectral signature of ice clouds in the far-infrared region: Single-scattering calculations and radiative sensitivity study. *J. Geophys. Res.,* **108,** 4569, doi:10.1029/2002JD003291.

——, L. Bi, B. A. Baum, K.-N. Liou, G. W. Kattawar, M. I. Mishchenko, and B. Cole, 2013: Spectrally consistent scattering, absorption, and polarization properties of atmospheric ice crystals at wavelengths from 0.2 to 100 μm. *J. Atmos. Sci.,* **70,** 330–347, doi:10.1175/JAS-D-12-039.1.